

Water absorption/swelling pressure of powder bentonites and analogism on water molecular formation in bentonite

Hideo Komine¹

¹ Department of Civil and Environment Engineering, Waseda University, 3-4-1, Okubo, Shinjuku-ku, Tokyo 169-8555, Japan

ABSTRACT

This study investigated water absorption and swelling pressure characteristics in a bentonite-based buffer from an unsaturated state to saturation from the viewpoint of material specifications such as the kinds of bentonite and dry density. From those experimentally obtained results, a database of water-diffusion coefficient and swelling-pressure for bentonites is presented. The author also discusses analogism on water molecular formation in bentonite.

Keywords: bentonite; montmorillonite; radioactive waste disposal; swelling; water absorption; water molecule

1 INTRODUCTION

The condition of bentonite-based buffer changes from unsaturated to saturated according to groundwater seepage at high-level radioactive waste disposal facilities. Therefore, the behavior of bentonite-based buffer must be investigated quantitatively under unsaturated conditions. This study investigated water absorption and swelling pressure characteristics in bentonite-based buffer from an unsaturated state to saturation in terms of material specifications of bentonite and dry density. Furthermore, this study presents all calculated saturation degrees of specimens at the end of the experiment using both amounts of water absorption and final water contents. From the above facts and results of earlier research, the author discusses analogism for molecular water formation in bentonite.

2 OUTLINE OF EXPERIMENT

This study uses experiments for measuring water absorption amounts and bentonite-based buffer swelling pressure. This section describes the materials used, experimental apparatus, and procedures.

2.1 Materials

Table 1 presents fundamental properties of the bentonite powders of three kinds used for this study. The author selected the three powders because of their different montmorillonite contents and exchangeable cation conditions. Bentonite A, actually Kunigel-V1, is a candidate buffer material in Japanese projects.

2.2 Experimental procedure

Figure 1 presents an example of the experiment showing the water absorption amount and swelling pressure with elapsed time.

Bentonite	A	B	C
Trade name	Kunigel-V1	Volclay	Kunibond
Particle shape	Powder	Powder	Powder
Type	Sodium	Sodium	Calcium
Density of soil particles (Mg/m ³)	2.79	2.84	2.71
Liquid limit (%)	458.1	565.0	128.7
Plastic limit (%)	23.7	47.2	38.4
Plastic index	434.4	517.8	90.3
Montmorillonite content (%)	57	71	84
CEC (meq./g)	1.166	1.054	0.795
EXC _{Na} (meq./g)	0.631	0.572	0.119
EXC _{Ca} (meq./g)	0.464	0.328	0.585
EXC _K (meq./g)	0.030	0.026	0.019
EXC _{Mg} (meq./g)	0.041	0.128	0.072

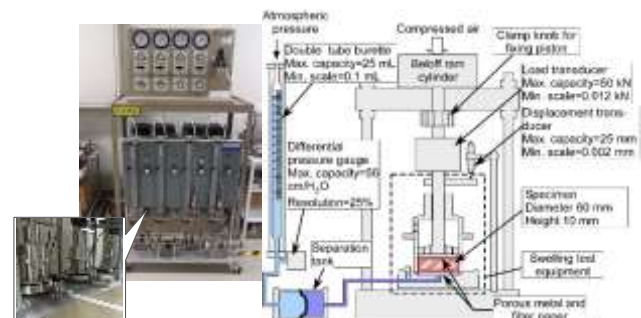


Fig. 1. Experiment apparatus.

This experiment measured the water absorption amount using a double tube burette and a differential pressure gauge at prescribed time intervals. In addition, the swelling pressure was measured by the load transducer. The minute vertical displacement of the specimen was

Table 1. Fundamental properties of bentonite

measured using the displacement transducer as presented in Fig. 1.

3 WATER ABSORPTION AND SWELLING PRESSURE OF BENTONITES

Figure 2 presents relations of the water absorption amount into a specimen and the swelling pressure per unit of elapsed time for sodium-type bentonite A. Regarding the relation between the amount of water absorption into the specimen and elapsed time, the water absorption amount into the specimen, Q , can be evaluated as a linear function of the square root of elapsed time as in Eq. (1) if the water-absorbing behavior is analogous to water-diffusion phenomena in the specimen (Komine et al., 2018).

$$Q = Q_0 - b = a\sqrt{t} \quad (1)$$

Therein, Q_0 represents the amount of inflow water measured by the double tube burette presented in Fig. 1, which includes the amount of absorbed water in the porous metal, filter paper, and the pipes between the double tube burette and the bottom of the specimen; also, a is the amount of water absorption per the unit of square root of time ($\text{mL}/\sqrt{\text{min}}$). t represents the elapsed time from the starting of water supply, b can be assumed as the amount of absorbed water in the porous metal, filter paper, and pipes between the double tube burette and the bottom of the specimen. Therefore, the water absorption into the specimen is calculable by Eq. (1). Nevertheless, it is impossible to confine the volume change of specimen completely. Therefore, the dry density of the specimen is corrected using Eq. (2)

$$\rho_{d0} = \frac{m_s}{A \times (H_0 + \Delta d)} \times 100 \quad (2)$$

In that equation, ρ_{d0} denotes the corrected dry density (Mg/m^3), m_s stands for the dry mass of specimen (g), A signifies the cross-section area of specimen (mm^2), H_0 expresses the specimen height (mm), and Δd represents the vertical displacement of the specimen (mm).

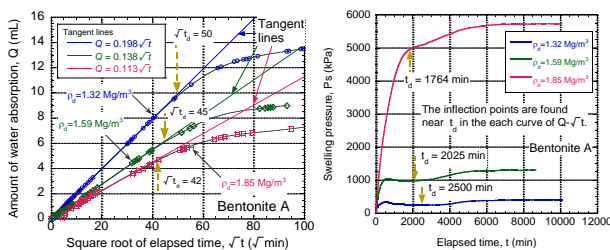


Fig. 2. Experiment results of the Bentonite A.

The left panel of Fig. 2 shows that water absorption amount Q into the specimen is directly proportional to the square root of elapsed time from $t=0$ to t_d . Results in both panels of Fig. 2 show an inflection point in the

relation of swelling pressure and elapsed time at t_d .

Figs. 3 and 4 show the obtained results for Bentonites B and C. Similarly to results for Bentonite A, Q is directly proportional to the square root of elapsed time from $t=0$ to t_d for Bentonites B and C.

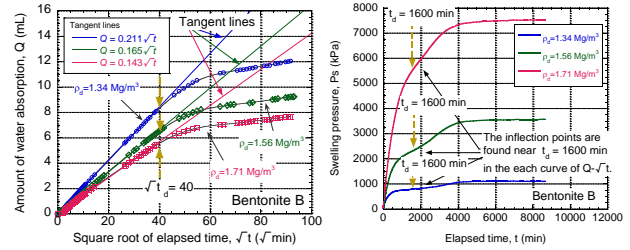


Fig. 3. Experiment results for Bentonite B.

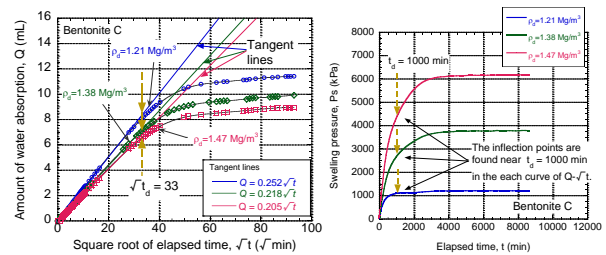


Fig. 4. Experiment results for Bentonite C.

At $t=0$ to t_d , water migration in the bentonite-based buffer specimen can be regarded as diffusion of water molecules because Q is directly proportional to the square root of elapsed time. After $t=t_d$, the degree of saturation is regarded as almost 100%. For that reason, water migration in the bentonite-based buffer specimen can be regarded as hydraulic conduction according to Darcy's law.

The initial air-void volume in a specimen is calculable from the dry density, water content, and specimen volume in the initial condition. From those values and measured inflow water amounts at t_d of each bentonite shown in Figs. 2–4, the degree of saturation at t_d is calculable as presented in Table 2. Results shown in Table 2 indicate that the degrees of saturation at t_d for bentonites A, B, and C are around 90%. Therefore, water migration in the bentonite-based buffer specimen can be regarded as diffusion of water molecules at the initial condition to t_d of about 90%. At t_d of about 90%, water migration is regarded as acting dominantly as hydraulic conduction (Komine, 2008, 2010).

From the respective relations between swelling pressure and elapsed time for bentonites A–C shown in the right panels of Figs. 2–4, inflection points can be confirmed clearly at t_d in sodium-type bentonites A and B. For calcium-type bentonite C, with less swelling than sodium-type bentonite A or B, the swelling pressure curve is inflected slightly.

Table 2. Relations of initial void volume (V_{a0}), inflow water amount (Q at t_d) and degree of saturation (S_r at t_d) at t_d

Bentonite ρ_{d0} (Mg/m ³)	w_0 (%)	S_{r0} (%)	V_{a0} (cm ³)	Q at t_d (cm ³)	S_r at t_d (%)
A	1.32	8.37	20.97	11.70	10.0
	1.59	8.47	31.31	8.41	6.5
	1.85	8.07	44.31	5.35	4.5
B	1.34	11.24	28.52	10.59	8.5
	1.56	11.28	39.04	7.90	6.5
	1.71	11.24	48.31	5.86	5.0
C	1.21	14.30	31.26	10.79	8.5
	1.38	14.72	41.39	8.21	7.0
	1.47	14.30	45.94	7.00	6.2

Results show that the generative behavior of swelling pressure varies according to the change of water migration in the specimen from water diffusion to hydraulic conduction. Komine and Ogata (1994) also reported inflection points in the curves of swelling pressure versus elapsed time. The inflection point probably originates in alternation of the void structure in the bentonite-based buffer caused by water migration. The alternation of water migration from water diffusion to hydraulic conduction results from the void structure alternation in bentonites.

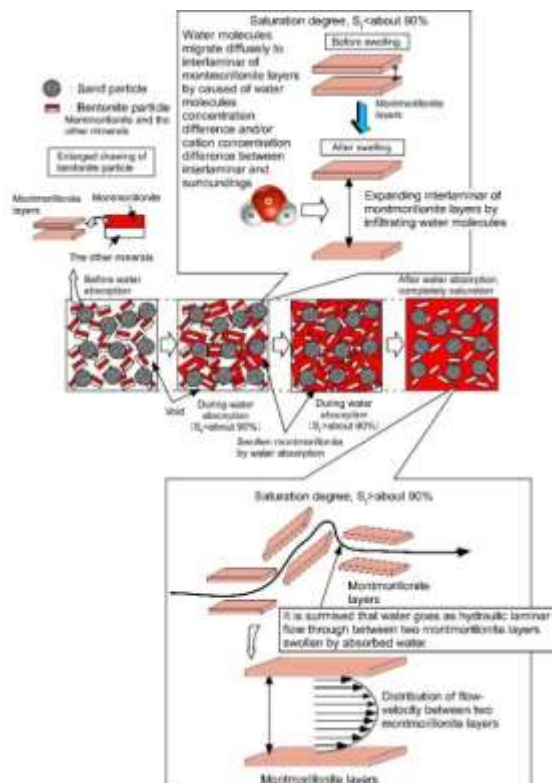


Fig. 5. Dominant mechanism of water absorption characteristics of bentonite-based buffer.

Based on the discussion presented above for the bentonite-based buffer, the dominant mechanism of water absorption characteristics is shown in Fig. 5.

4 ANALOGISM ON MOLECULAR WATER FORMATION IN BENTONITE

The previous section described and explained water absorption and swelling pressure of powder bentonites. Moreover, the dominant mechanism of water absorption characteristics of bentonite-based buffer was considered. As described in this section, the condition and/or formation of water molecular between montmorillonite layers shown in the right panel of Fig. 5 were inferred in terms of the degree of specimen saturation, which is calculable using the amount of water absorption and the water content at the end of the experiment.

Table 3 shows the degree of saturation calculated using water absorption and water content amounts at the end of the experiment for all specimens shown in Table 2.

Table 3. Specimen conditions for water absorption experiments and the saturation degree at the end of the experiment

	Bentonite A			Bentonite B			Bentonite C		
Case	A-1	A-2	A-3	B-1	B-2	B-3	C-1	C-2	C-3
ρ_d	1.32	1.59	1.85	1.34	1.56	1.71	1.21	1.38	1.47
w_0	8.37	8.47	8.07	11.24	11.28	11.24	14.30	14.72	14.30
S_{r-0}	20.97	31.31	44.31	28.52	39.04	48.31	31.26	41.39	45.94
Q_{final}	13.52	8.99	7.29	12.96	9.61	8.40	12.11	10.22	9.36
w_{final}	42.48	29.42	23.52	44.12	33.86	28.24	51.60	39.10	37.85
$S_{r-Qfinal}$	112.0	104.7	120.2	116.0	113.2	122.5	108.4	114.4	118.2
$S_{r-wfinal}$	105.7	108.8	129.7	111.6	116.4	121.3	112.7	109.6	120.8

Notation: ρ_d , dry density (Mg/m³); w_0 , initial water content (%); S_{r-0} , saturation degree at initial condition (%); Q_{final} , water absorption amount at the end of the experiment (cm³); w_{final} , water content at the end of the experiment (%); $S_{r-Qfinal}$, saturation degree calculated using the water absorption amount at the end of the experiment (%); $S_{r-wfinal}$, saturation degree calculated using water content at the end of the experiment (%)

Figure 6 presents relations between the saturation degree calculated using water contents at the end of the experiment and the saturation degree calculated using the water absorption amount at the end of the experiment. The results showed that the calculated saturation degrees might be almost equal and have a single meaning. Therefore, both calculated saturation degrees at the end of the experiment are regarded as reproducible and reliable. Moreover, some experiment cases exist in which the degree of saturation at the end of the experiment is greater than 120%, as shown in cases A-3, B-3, and C-3 in Table 3. The calculated saturation degree greater than 100% results from the assumption that the pore-water density in bentonite-based buffer is 1.0 Mg/m³: the same as that for free-water. From the discussion presented above, the density of water between montmorillonite layers in bentonite-based buffer is regarded as around 1.2 Mg/m³ because the calculated saturation degree at the end of the experiment is around 120%.

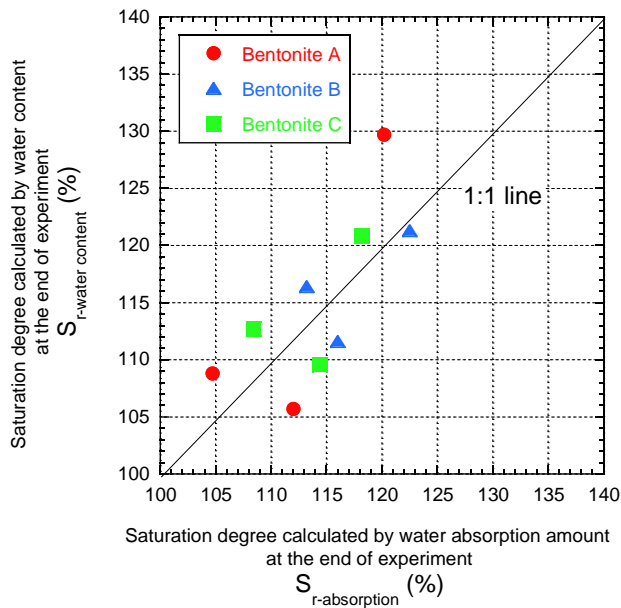


Fig. 6. Saturation degrees calculated using water content and using water absorption amount at the end of the experiment.

The above inference about the water density between montmorillonite described shows near agreement with other researchers' earlier reports, such as those of Martin (1962), Low (1976), Sposito and Prost (1982), Villar and Lloret (2004), and Jacinto et al. (2012). Martin (1962) described that the absorbed water around the montmorillonite mineral is regarded as around 1.16 Mg/m^3 in conditions of 100% relative humidity. This description nearly agrees with the prescribed inference.

The above analogism on molecular water formation in bentonite indicates that the water density in interlamellar montmorillonite is higher than that of free-water around montmorillonite minerals.

5 CONCLUSION

Experiments measuring water absorption and swelling pressure in bentonite-based buffer were done in an unsaturated state to a saturated state. The following conclusions were drawn from the experimentally obtained results and discussion.

Water absorption behaviors in various powder bentonites as buffer are analogous to water-diffusion from initial water content to around 90% saturation. At more than a 90% degree of saturation, the water migration is regarded as acting dominantly for hydraulic conduction. Furthermore, inflection points appear at around 90% saturation in relations between swelling-pressure and elapsed time. Results and discussion show the author's consideration of the water migration mechanism in bentonite from an unsaturated state to saturation. Factors dominating water migration in the buffer change according to alternation of the

microstructure by swelling in bentonite-based buffers.

Results show that all saturation of the specimen at the end of the experiment is greater than 100%, calculated using both the amount of water absorption and the final water content. The experimental results and earlier reported results (e.g. Martin, 1962) indicate that the water density in montmorillonite interlamellar is higher than that of free-water around montmorillonite minerals.

ACKNOWLEDGMENTS

This study was supported through funding by a Grant-in-Aid for Scientific Research (B) from the Japan Society for the Promotion of Science (JSPS). It has also been performed as a part of activities of the Research Institute of Sustainable Future Society, Waseda Research Institute for Science and Engineering, Waseda University. Furthermore, some research was conducted with support from "Human Resource Development and Research Program for Decommissioning of Fukushima Daiichi Nuclear Power Station" by the Japan Ministry of Education, Culture, Sports, Science and Technology. The author also thanks all members and students of the geotechnical laboratory, Waseda University, for their kind assistance and discussion.

REFERENCES

- Jacinto, A. C., Villar, M. V., and Ledesma, A. (2012). Influence of water density on the water-retention curve of expansive clays, *Geotechnique* 62(8), 657-667.
- Komine, H. (2008). Theoretical equations on hydraulic conductivities of bentonite based buffer and backfill for underground disposal of radioactive wastes, *Journal of Geotechnical and Geoenvironmental Engineering*, American Society of Civil Engineers (ASCE) 134(4), 497-508.
- Komine, H. (2010). Predicting hydraulic conductivity of sand-bentonite mixture backfill before and after swelling deformation for underground disposal of radioactive wastes, *Engineering Geology* 114, 123-134, doi: 10.1016/j.enggeo.2010.04.009.
- Komine, H. and Ogata, N. (1994). Experimental study on swelling characteristics of compacted bentonite, *Canadian Geotechnical Journal* 31(4), 478-490.
- Komine, H., Oyamada, T., Ozaki, T. and Iso, S. (2018). Discussion on water migration and swelling of compacted powder bentonites, *Journal of Japan Society of Civil Engineers Division C: Geotechnics* 74(1), 63-75. (in Japanese with English abstract)
- Low, P. F. (1976). Viscosity of interlayer water in montmorillonite, *Soil Science Society of America Journal* 40(4), 500-505.
- Martin, R. T. (1962). Adsorbed water on clay: a review, *Ninth National Conference on Clays and Clay Minerals* 28-70.
- Sposito, G., and Prost, R. (1982). Structure of water adsorbed onto smectites, *Chemical Reviews* 82(6), 554-573. doi: 10.1021/cr00052a001.
- Villar, M. V., and Lloret, A. (2004). Influence of temperature on the hydro-mechanical behaviour of a compacted bentonite, *Applied Clay Science* 26(1-4), 337-350.